Spectroscopic Distinction of Surface and Volume Ions in Cerium(III)- and Terbium(III)-Containing Core and Core/Shell Nanoparticles

Karsten Kömpe,*,† Olaf Lehmann,‡ and Markus Haase†

Institut für Physikalische Chemie, Universität Hamburg, Grindelallee 117, 22146 Hamburg, Germany, and Institut für Chemie, Universität Osnabrück, Barbarastrasse 7, 49069 Osnabrück, Germany

Received April 13, 2006. Revised Manuscript Received June 23, 2006

Core and core/shell Tb^{3+}-doped $CePO_4$ and $LaPO_4$ nanoparticles have been prepared in an organic solvent mixture. The particles were characterized by X-ray diffraction (XRD), UV−vis absorption spectra, luminescence spectra, and lifetimes. It is shown that the luminescence spectra of Ce^{3+} and Tb^{3+} ions at the particle surface differ from those located in the interior of the nanocrystals. The emission of cerium surface ions is red-shifted compared to the emission of ions in the particle center. Tb^{3+} ions at the surface display strongly broadened emission lines, indicating a variety of different surface sites.

Introduction

For most potential applications of luminescent nanocrystals a high quantum efficiency is required.[1−4] Although nanocrystals provide a rigid crystalline environment for dopant ions, the luminescence quantum yield of doped nanocrystals ("nanophosphors") is usually much lower compared to the corresponding bulk materials. At technologically relevant doping levels this is caused mainly by energy migration to the particle surface followed by radiationless relaxation to the ground state.[5−7] These energy-loss processes at the particle surface can be significantly reduced by coating the particles with a material that grows epitactically on the nanocrystal material and which provides a barrier for energy migration to the outer surface of the shell.

One example for such materials is $LaPO_4$ codoped with 45% Ce^{3+} and 15% Tb^{3+}. In this material fast energy migration occurs between adjacent Ce^{3+} ions as well as between Ce^{3+} and Tb^{3+} ions, leading to efficient Tb^{3+} emission upon UV excitation of the Ce^{3+} ion. The bulk material has therefore been used as an efficient emitter of green light in fluorescent tubes.[8] Bulk $LaPO_4$:Ce,Tb shows high chemical stability, even against the mercury discharge inside the lamp, and exhibits a quantum efficiency of over 90%.[9] Recently it was shown that the quantum yield of the corresponding nanomaterial can be improved significantly by growing a shell of pure $LaPO_4$ on $LaPO_4$:Ce,Tb core particles.[10]

In this paper we will discuss the luminescence properties of Ce^{3+} and Tb^{3+} ions at the surface and those in the interior of lanthanide phosphate nanoparticles.

All nanocrystals employed in this paper are fully redispersible in organic solvents to give clear and transparent colloidal solutions. The following abbreviations are used throughout the text:

$CePO_4$, $CePO_4$:Tb^{3+} (2%), and $CePO_4$:Tb^{3+} (25%) core particles refer to pure cerium phosphate nanoparticles and cerium phosphate particles doped with 2% and 25% terbium, respectively. Coating the pure $CePO_4$ (core) particles with a shell of $TbPO_4$ (3:1) or $LaPO_4$ (1:3) leads to core/shell nanoparticles, referred to as $CePO_4$/$TbPO_4$ or $CePO_4$/$LaPO_4$. An additional $LaPO_4$ shell leads to $CePO_4$/$TbPO_4$/$LaPO_4$ (3:1:12) particles. Analogous abbreviations are used for nanocrystals based on $LaPO_4$ cores rather than $CePO_4$ cores.

Experimental Section

Synthesis. The synthesis of all nanoparticles were carried out in high boiling coordinating solvents according to a modified procedure:[11] To a clear solution of the lanthanide chloride hydrates (10 mmol of lanthanide chlorides in total, e.g. 7.5 mmol of $CeCl_3 \cdot 7H_2O$ with 2.5 mmol of $TbCl_3 \cdot 6H_2O$ for the $CePO_4$:Tb^{3+} (25%) nanoparticles) in approximately 10 mL of methanol pa was added 40 mmol of tributyl phosphate, and the methanol was subsequently distilled off with a rotary evaporator. A 30 mL volume of diphenyl ether was added, and the water was removed under reduced pressure

* To whom correspondence should be addressed. E-mail: karsten.koempe@uni-osnabrueck.de.
† Universität Osnabrück.
‡ Universität Hamburg.

(1) Colvin, V. L.; Schlamp, M. C.; Alivisatos, A. P. *Nature* **1994**, *370*, 354.
(2) Klimov, V. I.; Mikhailovsky, A. A.; Xu, S.; Hollingsworth, J. A.; Leatherdale, C. A.; Eisler, H. J.; Bawendi, M. G. *Science* **2000**, *290*, 314.
(3) Harrison, M. T.; Kershaw, S. V.; Burt, M. G.; Rogach, A. L.; Kornowski, A.; Eychmüller, A.; Weller, H. *Pure Appl. Chem.* **2000**, *72*, 314.
(4) Dubertret, B.; Skourides, P.; Norris, D. J.; Noireaux, V.; Brivanlou, A. H.; Libchaber, A. *Science* **2002**, *298*, 1759.
(5) Huignard, A.; Gacoin, Th.; Boilot, J.-P. *Chem. Mater.* **2000**, *12*, 1090.
(6) Riwotzki, K.; Meyssamy, H.; Kornowski, A.; Haase, M. *J. Phys. Chem. B* **2000**, *104*, 2824.
(7) Hebbink, G. A.; Stouwdam, J. W.; Reinhoudt, D. N.; van Veggel, F. C. J. M. *Adv. Mater.* **2002**, *14*, 1147.
(8) Hashimoto, N.; Takada, Y.; Sato, K.; Ibuki, S. *J. Lumin.* **1991**, *48*−*49*, 893.
(9) Smets, B. M. J. *Mater. Chem. Phys.* **1987**, *16*, 283.
(10) Kömpe, K.; Borchert, H.; Storz, J.; Lobo, A.; Adam, S.; Möller, T.; Haase, M. *Angew. Chem., Int. Ed* **2003**, *42*, 5513.
(11) Lehmann, O.; Meyssamy, H.; Kömpe, K.; Schnablegger, H.; Haase, M. *J. Phys. Chem. B* **2003**, *107*, 7449.

10.1021/cm060857g CCC: $33.50
Published on Web 08/04/2006

by slowly increasing the temperature from 20 to 100 °C. A 30 mmol amount of tridodecylamine and 7.0 mL of a dry 2 M solution of phosphoric acid in dihexyl ether were added, and the mixture was heated to 200 °C under dry nitrogen. After 16 h the heating was stopped and the solution was allowed to cool.

The $LaPO_4$, 1:3 ($TbPO_4$, 3:1), shells were synthesized as follows: To a solution of 7.5 mmol of $LaCl_3 \cdot 7H_2O$ (2.5 mmol of $TbCl_3 \cdot 6H_2O$) in 10 mL of methanol pa was added 30 (10) mmol of tributyl phosphate, and the methanol was subsequently removed with a rotary evaporator. Diphenyl ether (20 mL) was added, and the water was distilled off as described above. After being mixing with 22.5 (7.5) mmol of tridodecylamine, this solution was filled into a dropping funnel. A mixture of 5.25 (1.75) mL of 2 M phosphoric acid solution in dihexyl ether and 20 mL of diphenyl ether was filled into another dropping funnel. These two solutions were added dropwise over a period of 2 h to a solution of the $LnPO_4$ nanoparticles in 50 mL of diphenyl ether, according to 2.5 (7.5) mmol of metal ions, kept under dry nitrogen at 200 °C. After 16 h the heating was stopped and the solution was allowed to cool.

$LaPO_4/TbPO_4$ (5%) nanoparticles were prepared by first synthesizing pure $LaPO_4$ nanocrystals in the same way as the other core particles. Then, a solution of 0.5 mmol of $TbCl_3 \cdot 6H_2O$ in 1.5 mL of diphenyl ether, 2 mmol of tributyl phosphate, and 1.5 mmol of tridodecylamine was prepared and the water removed as given above. This solution was loaded into a dropping funnel and added dropwise during 45 min to the reaction mixture of $LaPO_4$ particles which was kept at 200 °C under dry nitrogen. After 16 h at 200 °C the reaction mixture was allowed to cool.

Subsequently, the reaction mixtures were all treated in the same way to isolate the nanoparticles as dry powders: the reaction solution was mixed with 250 mL of methanol, and the precipitated product was separated from the liquid via centrifugation. The deposit was washed two times with methanol, and finally, the nanoparticles were dried. White powders of nanoparticles were obtained in gram amounts.

To redisperse the particles in methanol the dry powder was washed three times with a solution of HCl in methanol (~50 mM). The excess of HCl was removed by a two times washing of the particles with methanol. Dropwise adding of a solution of tetramethylammonium hydroxide in methanol (~25%) to the particles in about 5 mL of methanol finally gave clear and transparent solutions.

Characterization. X-ray diffraction patterns of the powder samples were recorded with a Philips X′pert system.

The luminescence spectra of nanoparticle solutions in methanol were measured with a Fluorolog-03 spectrometer (Jobin-Yvon). The measurements of absorption spectra were carried out with a double-beam Cary 6000i (Varian) spectrometer.

For the measurement of the fluorescence spectra of terbium, the nanoparticle powders were cooled to 30 K inside a closed cycle cryostat (Leybold) and were excited with a Continuum Sunlite EX OPO pumped by a Continuum Precision II Nd:YAG laser. The fluorescence light was dispersed with a TRIAX 320 monochromator (Jobin Yvon; 1800 groove grating) and detected with a nitrogen-cooled CCD 3000 camera (Jobin Yvon). Luminescence spectra were recorded by averaging the emission over at least 20 excitation pulses. Luminescence decay curves were recorded with a Hamamatsu R928 photomultiplier in combination with a digital oscilloscope (Tektronix TDS 3032B).

Results and Discussion

The nanoparticles investigated here were prepared in a coordinating solvent mixture with an excess of phosphoric acid as described previously.[11] The yields obtained after the synthesis indicate in all cases complete reaction of the lanthanide ions.

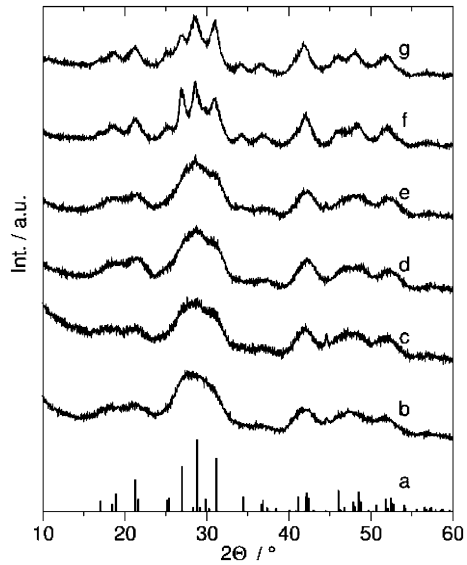

Figure 1. X-ray diffraction patterns of the different $CePO_4$ nanoparticles: (a) line positions of the monazite $CePO_4$ lattice (PDF 83-0652); (b) $CePO_4$; (c) $CePO_4$:Tb(2%); (d) $CePO_4$:Tb (25%); (e) $CePO_4/TbPO_4$; (f) $CePO_4/TbPO_4/LaPO_4$; (g) $CePO_4/LaPO_4$.

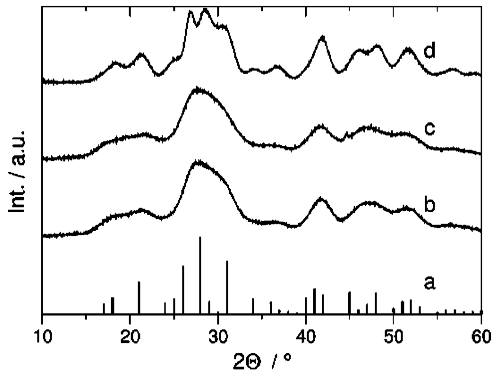

Figure 2. X-ray diffraction patterns of the $LaPO_4$ nanoparticles: (a) line positions of the monazite $LaPO_4$ lattice (PDF 84-0600); (b) $LaPO_4/TbPO_4$ (5%); (c) $LaPO_4$:Tb (1%); (d) $LaPO_4$:Tb (1%)/$LaPO_4$.

The X-ray powder diffraction (XRD) patterns of all systems examined are summarized in Figures 1 and 2 and are similar to those published for $CePO_4$:Tb^{3+}, $CePO_4$:Tb^{3+}/$LaPO_4$ core/shell, and $LaPO_4$ nanoparticles.[10,11] The particle sizes have been estimated from the width of the diffraction lines by using the Debye−Scherrer formula, which yields mean particle diameters of approximately 4−5 and 7−9 nm for core and core/shell particles, respectively. Only in the case of terbium-coated particles the increase of the particle diameter is negligible, due to the small amount of terbium shell material employed (mass ratio of 3:1 for the core and shell components).

The peak positions and intensities are in accord with the literature values for the monoclinic monazite phase of the corresponding bulk materials. Since the unit cell parameters are very similar for both materials, $LaPO_4$ grows epitactically on $CePO_4$ core particles, as discussed earlier.[10]

Figure 3 displays the Ce^{3+} emission spectra of dilute colloidal solutions of the different Ce^{3+}-containing nano-

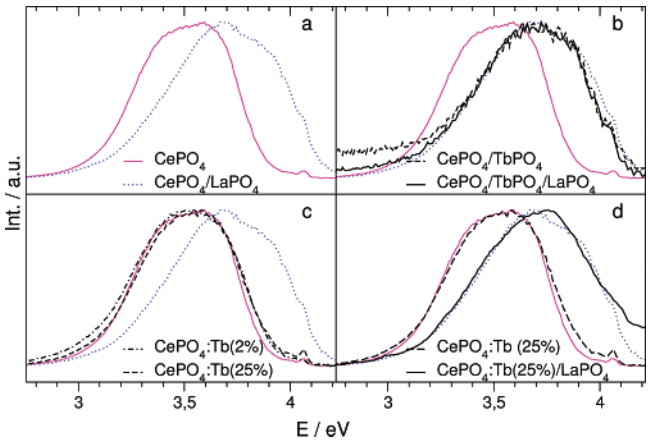

Figure 3. Normalized luminescence spectra of the Ce^{3+} emission of different nanoparticles under excitation with light of the energy of 4.5 eV (275 nm).

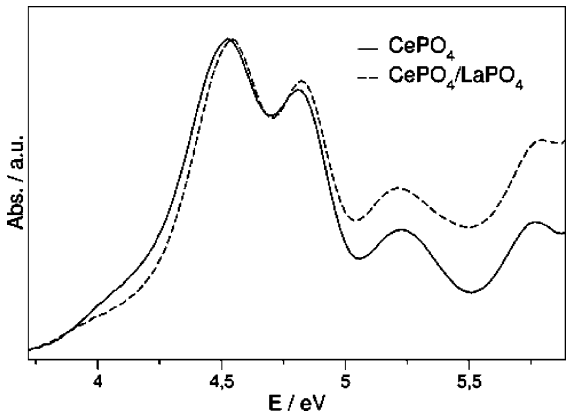

Figure 4. Absorption spectra of $CePO_4$ and $CePO_4/LaPO_4$ nanoparticles.

particles. In all cases, the 4f−5d transition of the nanocrystals was excited at 275 nm (4.5 eV), resulting in a stokes-shifted broad emission band with a full-width at half-maximum of approximately 0.5 eV. The spectra in Figure 3 have been normalized, since the intensity of the emission strongly depends on the composition and the structure (core or core/shell) of the nanocrystals as will be discussed below. While the shape of the emission band is similar in all cases, its spectral position is not. However, in all cases the band is centered at one out of only two distinct positions: the luminescence of core particles is generally observed at approximately 3.5 eV whereas the luminescence of the core/shell particles is blue-shifted by approximately 0.2 eV and is centered at approximately 3.7 eV. This blue-shift is observed not only after coating pure $CePO_4$ core particles (Figure 3a) or doped $CePO_4$:Tb core particles (Figure 3c) with a $LaPO_4$ shell (Figure 3d) but also after the formation of a thin $TbPO_4$ surface layer around $CePO_4$ core particles (Figure 3b). Coating the latter $CePO_4/TbPO_4$ core/shell particles with an additional $LaPO_4$ shell, however, did not further increase the blue-shift (Figure 3b).

In contrast, no blue-shift is observed if the Tb^{3+} ions are doped into the crystal lattice of $CePO_4$ core particles (Figure 3c) instead of being deposited onto their surface as a $TbPO_4$ layer. Even if the Tb^{3+} concentration of the doped $CePO_4$ nanocrystals is increased to 25%, i.e., to a value which approaches the overall chemical composition of the $CePO_4/TbPO_4$ core/shell particles, no strong blue-shift is observed (Figure 3c). These observations strongly indicate that the spectral position of the Ce^{3+} emission is connected to surface properties of the nanocrystals. In fact, the transition energy of the Ce^{3+} 4f−5d transition is known to depend on the crystal field strength.[12] Growth of a crystalline shell around the particles therefore will influence the crystal field strength at the Ce^{3+} surface ions.

For instance, if a $LaPO_4$ shell is grown epitactically onto a $CePO_4$ nanocrystal, the crystal field at Ce^{3+} surface sites is expected to become comparable to the crystal field at Ce^{3+} sites in the center of the nanocrystal, because the lattice constants of $LaPO_4$ and $CePO_4$ are almost identical and the electronic properties of the La^{3+} ion and the Ce^{3+} ion are similar. Therefore, the absorption and the luminescence spectra of $CePO_4/LaPO_4$ core/shell particles will resemble mainly the properties of Ce^{3+} volume sites. In fact, the emission of those core/shell particles at 3.7 eV lies at the same value as in cerium-doped $LaPO_4$ bulk material.[13] The corresponding spectra of $CePO_4$ core particles, on the other hand, will display contributions of the Ce^{3+} surface sites, as for particles with a diameter of 5 nm approximately 25% of all Ce^{3+} ions are located at the particle surface. The Ce^{3+} absorption of $CePO_4$ core particles is weakly red-shifted with respect to the absorption of $CePO_4/LaPO_4$ core/shell particles, indicating that the core particles contain a quantity of Ce^{3+} sites with smaller crystal field strength (Figure 4). However, the observed spectral shift is much more pronounced in the luminescence spectra (Figure 3a), because energy migration between adjacent Ce^{3+} ions is known to be very fast in highly doped Ce^{3+} systems. Therefore, the excitation energy is expected to rapidly migrate from the excited state of Ce^{3+} in volume sites to the excited states of Ce^{3+} on surface ions, which lie at lower energy (Figure 5). Consequently, $CePO_4$ core particles display an emission which originates predominantly from Ce^{3+} surface sites, resulting in a red-shift of the luminescence band compared to core/shell particles (Figure 3a).

In the $CePO_4/TbPO_4$ particles the above-mentioned fast energy migration via adjacent Ce^{3+} ions finally leads to energy transfer and excitation of the terbium ions on the surface of the $CePO_4$ core (Figure 5). Since the surface Ce^{3+} sites and the Tb^{3+} ions are direct neighbors, energy transfer between them is very efficient and the emission of the Ce^{3+} surface sites is strongly quenched. As a consequence, the Ce^{3+} luminescence of $CePO_4/TbPO_4$ particles originates mainly from Ce^{3+} volume sites. An additional $LaPO_4$ shell on top of the $TbPO_4$ shell has therefore no influence on the Ce^{3+} emission which is centered at approximately 3.7 eV independent of the presence or absence of a $LaPO_4$ shell (Figure 3b).

In terbium-doped $CePO_4$ particles fast energy transfer is expected to take place from Ce^{3+} ions to Tb^{3+} ions as well as from Ce^{3+} volume sites to Ce^{3+} surface sites (Figure 5). The former leads to strong quenching of the Ce^{3+} emission while the latter is responsible for its red-shift. If doped

(12) Dorenbos, P. *Phys. Rev. B* **2001**, *64*, 125117.

(13) Blasse, G.; Bril, A. *J. Chem. Phys.* **1967**, *47*, 5139.

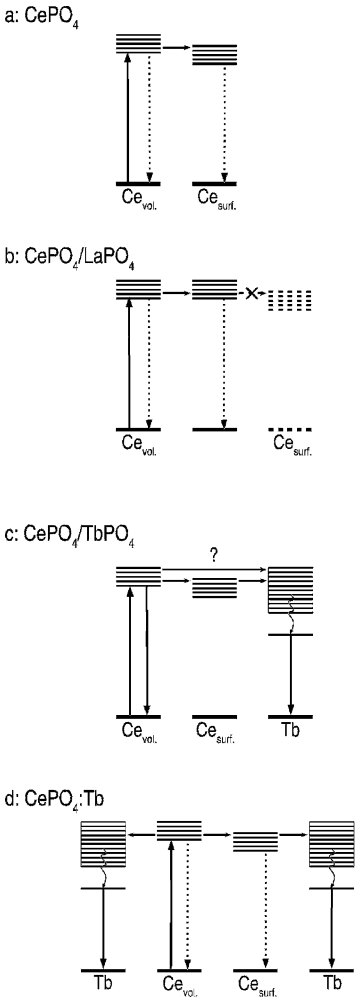

Figure 5. Schematic energy level diagram for (a) pure $CePO_4$, (d) doped $CePO_4$, and (b, c) core/shell $CePO_4$ nanoparticles.

particles are coated with a $LaPO_4$ shell, the Ce^{3+} surface sites are converted to interface sites which emit at a similar energy as the volume sites, as was the case without terbium. Yet, the $LaPO_4$ shell causes a blue-shift of the Ce^{3+} luminescence (Figure 3d), in contrast to the $CePO_4/TbPO_4/LaPO_4$ core/shell particles (Figure 3b).

Figure 6 shows the emission spectra of different nanoparticle solutions, all of which have been adjusted to the same optical density of 0.1 at the excitation energy of 4.43 eV. The emission spectra of Tb^{3+}-doped $CePO_4$ nanoparticles display four strong lines between 1.9 and 2.6 eV which correspond to transition between the $^5D_4$ state and the ^7F_J states ($J = 6, 5, 4, 3$) of Tb^{3+}. The lines are broadened due to the crystal field splitting of these levels. Due to the energy transfer from Ce^{3+} to Tb^{3+}, the Ce^{3+} luminescence in these samples is quenched compared to the emission of pure $CePO_4$ nanoparticles, slightly in the case of the $CePO_4$:Tb^{3+} (2%) particles and stronger in all other cases. Similar to the corresponding bulk materials, the energy transfer from Ce^{3+} to Tb^{3+} is enhanced if the Tb^{3+} content of the samples is increased from 2% to 25%, resulting in a stronger quenching of the Ce^{3+} emission and an increased intensity of the Tb^{3+} emission. Figure 6 shows also that the quenching of the Ce^{3+} emission is equally strong for the $CePO_4$:Tb^{3+} and $CePO_4/TbPO_4$ particles, both containing 25% terbium. This is remarkable because the mean distance between Ce^{3+} and

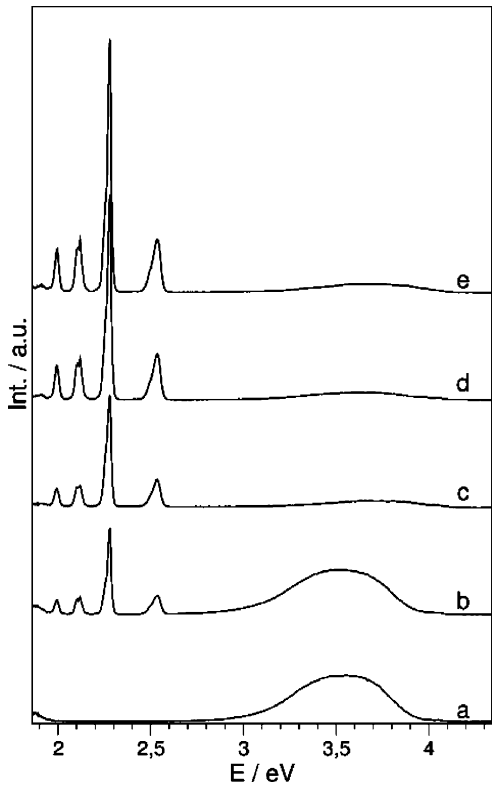

Figure 6. Luminescence spectra of the different nanoparticle solutions of identical optical density at the excitation energy of 4.43 eV: (a) $CePO_4$; (b) $CePO_4$:Tb^{3+} (2%); (c) $CePO_4/TbPO_4$ (25%); (d) $CePO_4$:Tb^{3+} (25%); (e) $CePO_4/TbPO_4/LaPO_4$.

Tb^{3+} is larger in the case of the $CePO_4/TbPO_4$ core/shell particles and indicates an exciton diffusion length in $CePO_4$ nanocrystals of more than 25 Å, i.e., the mean radius of the $CePO_4$ core particles. The quantum yield of the Tb^{3+} emission, however, is about 50% lower for the $CePO_4/TbPO_4$ particles. This is expected, because concentration quenching is likely to occur inside the $TbPO_4$ shell as is known for many bulk materials containing a high concentration of Tb^{3+}. In the case of our nanoparticles additional quenching can occur due to the proximity of the $TbPO_4$ shell to high-frequency vibrations of the organic surface ligands. In fact, Figure 6 shows that the quantum yield of the Tb^{3+} emission increases when the distance to the organic ligands is increased by a $LaPO_4$ shell on top of the $TbPO_4$ layer.

To obtain more insight in the distribution of Tb^{3+} ions inside the doped nanoparticles and core/shell nanoparticles, we investigated their Tb^{3+} luminescence spectra by direct excitation of the terbium $^7F_6-{}^5D_4$ transition at low temperature (30 K). Similar measurements had been performed earlier on europium-doped $LaPO_4$ nanocrystals.[14,15] In contrast to the corresponding Eu^{3+} states, the $^7F_6$ and $^5D_4$ levels of the Tb^{3+} ions are strongly split by the crystal field.[16] Therefore, selective excitation of different Tb^{3+} sites in one sample is more difficult to achieve than for europium-doped materials. Nevertheless, Tb^{3+} ions at the particle surface can

(14) Lehmann, O.; Kömpe, K.; Haase, M. *J. Am. Chem. Soc.* **2004**, *126*, 14935.
(15) Sudarsan, V.; van Veggel, F. C. J. M.; Herring, R. A.; Raudsepp, M. *J. Mater. Chem.* **2005**, *15*, 1332.
(16) Blasse, G.; Grabmaier, B. C. *Luminescent Materials*: Springer: Berlin, 1994.

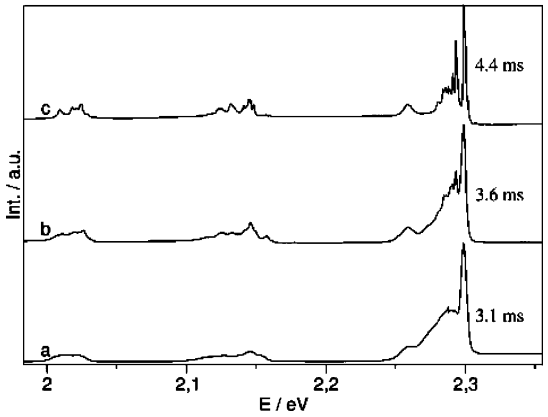

Figure 7. Tb^{3+} luminescence spectra under excitation with light of the energy of 2.55 eV: (a) $LaPO_4/TbPO_4$ (5%); (b) $LaPO_4$:Tb (1%); (c) $LaPO_4$:Tb/$LaPO_4$. The more Tb^{3+} ions are located in the interior of the particles, the narrower the peaks become and the longer the luminescence lifetime (indicated right) gets.

be distinguished spectroscopically from those in the particle center by their different crystal field splitting. This is shown in Figure 7 where the luminescence spectra of $LaPO_4/TbPO_4$ (5%), $LaPO_4$:Tb^{3+} (1%), and $LaPO_4$:Tb^{3+} (1%)/$LaPO_4$ nanoparticles are compared. The results are very similar to those obtained with the corresponding europium-doped samples: $LaPO_4$:Tb^{3+} (1%)/$LaPO_4$ core/shell nanoparticles display a luminescence spectrum with well-defined crystal-field splitting of the narrow luminescence lines. This shows that the crystal field is very similar for most Tb^{3+} ions, as it is the case in bulk $LaPO_4$:Tb. This is expected, because the Tb^{3+} surface sites are converted into volume sites by growing the $LaPO_4$ shell, thereby reducing the number of different Tb^{3+} sites in the material. In contrast, $LaPO_4/TbPO_4$ (5%) particles display broad emission lines, indicating that the simultaneous emission of a large number of different sites at the particle surface is observed. These sites are either excited simultaneously by the laser light source or are connected by energy-transfer processes, as expected for a layer with high terbium concentration. Finally, the emission spectrum of $LaPO_4$:Tb^{3+} (1%) particles without a $LaPO_4$ shell can be interpreted as the intermediate case, with surface sites and volume sites being present in one sample. The mean luminescence lifetimes (monoexponential fit) of the Tb^{3+} emission support this conclusion. The more terbium is located on the surface of the particles, the shorter are the observed lifetimes, as expected if quenching processes are most efficient at the particle surface.

Conclusions

The luminescent properties of Ce^{3+} and Tb^{3+} ions in doped $CePO_4$ and $LaPO_4$ core and core/shell nanoparticles do not only differ with respect to their quantum yields. The Ce^{3+} emission in core nanoparticles is red-shifted compared to core/shell particles. Energy transfer from the excited states in volume sites to surface sites is responsible for this observation. Due to the large surface/volume ratio, the smaller crystal field strength on surface Ce^{3+} ions takes the dominant role in the emission properties of core nanoparticles. The emission of Ce^{3+} ions in core/shell nanoparticles therefore only corresponds to excited volume sites and is blue-shifted compared to core nanoparticles.

In the case of Tb^{3+}-doped core nanoparticles broad emission lines indicate simultaneous emission from sites with different crystal field splitting whereas narrow luminescence lines in core/shell particles are resulting from the well-defined crystal-field splitting of volume ions only.

Acknowledgment. This work was partly funded by the BMBF.

CM060857G